

**UCLA**

**UCLA Previously Published Works**

**Title**

Glucagon Receptor Antagonist for Heart Failure With Preserved Ejection Fraction.

**Permalink**

<https://escholarship.org/uc/item/37d4s9rd>

**Authors**

Gao, Chen

Xiong, Zhaojun

Liu, Yunxia

et al.

**Publication Date**

2024-07-16

**DOI**

10.1161/circresaha.124.324706

Peer reviewed

## ORIGINAL RESEARCH

## Glucagon Receptor Antagonist for Heart Failure With Preserved Ejection Fraction

Chen Gao, Zhaojun Xiong, Yunxia Liu<sup>1</sup>, Meng Wang, Menglong Wang<sup>1</sup>, Tian Liu, Jianfang Liu<sup>1</sup>, Shuxun Ren<sup>1</sup>, Nancy Cao, Hai Yan, Daniel J. Drucker<sup>1</sup>, Christoph Daniel Rau<sup>1</sup>, Tomohiro Yokota, Jijun Huang<sup>1</sup>, Yibin Wang<sup>1</sup>

**BACKGROUND:** Heart failure with preserved ejection fraction (HFpEF) is an emerging major unmet need and one of the most significant clinic challenges in cardiology. The pathogenesis of HFpEF is associated with multiple risk factors. Hypertension and metabolic disorders associated with obesity are the 2 most prominent comorbidities observed in patients with HFpEF. Although hypertension-induced mechanical overload has long been recognized as a potent contributor to heart failure with reduced ejection fraction, the synergistic interaction between mechanical overload and metabolic disorders in the pathogenesis of HFpEF remains poorly characterized.

**METHOD:** We investigated the functional outcome and the underlying mechanisms from concurrent mechanic and metabolic stresses in the heart by applying transverse aortic constriction in lean C57Bl/6J or obese/diabetic B6.Cg-Lep<sup>ob</sup>/J (ob/ob) mice, followed by single-nuclei RNA-seq and targeted manipulation of a top-ranked signaling pathway differentially affected in the 2 experimental cohorts.

**RESULTS:** In contrast to the post-trans-aortic constriction C57Bl/6J lean mice, which developed pathological features of heart failure with reduced ejection fraction over time, the post-trans-aortic constriction ob/ob mice showed no significant changes in ejection fraction but developed characteristic pathological features of HFpEF, including diastolic dysfunction, worsened cardiac hypertrophy, and pathological remodeling, along with further deterioration of exercise intolerance. Single-nuclei RNA-seq analysis revealed significant transcriptome reprogramming in the cardiomyocytes stressed by both pressure overload and obesity/diabetes, markedly distinct from the cardiomyocytes singularly stressed by pressure overload or obesity/diabetes. Furthermore, glucagon signaling was identified as the top-ranked signaling pathway affected in the cardiomyocytes associated with HFpEF. Treatment with a glucagon receptor antagonist significantly ameliorated the progression of HFpEF-related pathological features in 2 independent preclinical models. Importantly, cardiomyocyte-specific genetic deletion of the glucagon receptor also significantly improved cardiac function in response to pressure overload and metabolic stress.

**CONCLUSIONS:** These findings identify glucagon receptor signaling in cardiomyocytes as a critical determinant of HFpEF progression and provide proof-of-concept support for glucagon receptor antagonism as a potential therapy for the disease.

**GRAPHIC ABSTRACT:** A graphic abstract is available for this article.

**Key Words:** cardiology ■ heart failure ■ hypertension ■ risk factors ■ stroke volume

Heart failure is a leading cause of death worldwide.<sup>1</sup> Among heart failure patients, a significant portion of them present with preserved ejection fraction (HFpEF) based on echocardiogram.<sup>2,3</sup> In general, patients with HFpEF have comparable morbidity and mortality as

patients with heart failure with reduced ejection fraction (HFrEF).<sup>4</sup> However, they are largely refractory to the current standard therapies, and the total number of HFpEF cases is increasing globally, reaching nearly 50% of the total heart failure population in some regions.<sup>5</sup> Given this

Correspondence to: Chen Gao, PhD, Department of Pharmacology and Systems Physiology, University of Cincinnati, Cincinnati, OH, Email gaoc3@ucmail.uc.edu; or Yibin Wang, PhD, Signature Program in Cardiovascular and Metabolic Diseases, Duke-NUS Medical School and National Heart Center of Singapore, 8 College Rd, Level 8, Singapore 169857, and Department of Medicine, Duke University School of Medicine, Durham, NC 27710, Email yibinwang@Duke-nus.edu.sg  
Supplemental Material is available at <https://www.ahajournals.org/doi/suppl/10.1161/CIRCRESAHA.124.324706>.

For Sources of Funding and Disclosures, see page XXX.

© 2024 American Heart Association, Inc.

Circulation Research is available at [www.ahajournals.org/journal/res](http://www.ahajournals.org/journal/res)

## Novelty and Significance

### What Is Known?

- Heart failure with preserved ejection fraction (HFpEF) is a complex disease characterized by normal ejection fraction but profound diastolic dysfunction, cardiac hypertrophy, and fibrosis.
- HFpEF is a multi-factorial disease commonly associated with numerous risk factors, including aging, metabolic disorders, and hypertension.
- Glucagon is a potent regulator of glucose homeostasis and insulin signaling, mostly through its receptor-mediated regulation of glucose metabolism and insulin secretion in the liver and pancreas.

### What New Information Does This Article Contribute?

- Mechanical stress led to divergent pathological outcomes in lean versus diabetic/obese mice. While the lean mice developed a prototypic cardiac phenotype of heart failure with reduced ejection fraction, the diabetic/obese mice showed characteristic features of HFpEF.
- Bulk and single-nuclei transcriptome data sets identified unique molecular signatures in cardiomyocytes associated with pressure overload, metabolic disorders, and the combination with particular differences in insulin and glucagon signaling.
- We showed that targeted inhibition of glucagon signaling ameliorated the pathogenic features of HFpEF.

HFpEF is an emerging disease with limited effective therapies relative to traditional heart failure with reduced ejection fraction. HFpEF is significantly associated with multiple risk factors, including aging, metabolic disorders such as diabetes and obesity, and hypertension. While each of these individual risk factors has been extensively studied for their contributions to cardiac pathology, their synergistic effects on the pathogenesis of HFpEF remain poorly studied. In this study, we found mechanical overload in lean mice developed prototypical features of heart failure with reduced ejection fraction, but in obese/diabetic mice, it promoted pathological features of HFpEF. Transcriptome profiling from these hearts identified insulin signaling and glucagon signaling as the top molecular pathways that differentiate heart failure with reduced ejection fraction versus HFpEF cardiomyocytes. Using a glucagon receptor antagonist and a mouse line of cardiomyocyte-specific knockout of the mouse glucagon receptor gene (*gcgr*), we demonstrated that the glucagon receptor antagonist significantly ameliorated the pathogenesis of HFpEF, indicating its potential as a therapy for the disease.

### Nonstandard Abbreviations and Acronyms

<b>αMHC-MCM</b>	alpha myosin heavy chain-mer-cre-mer
<b>AMPK</b>	adenosine monophosphate activated protein kinase
<b>Col1a1</b>	collagen 1 alpha 1
<b>Col3a1</b>	collagen 3 alpha 1
<b>GCGR</b>	glucagon receptor
<b>GLP-1</b>	glucagon-like peptide-1
<b>HFD</b>	high-fat diet
<b>HFpEF</b>	heart failure with preserved ejection fraction
<b>HFrEF</b>	heart failure with reduced ejection fraction
<b>IRE1α</b>	inositol-requiring enzyme 1 alpha
<b>L-NAME</b>	Nω-nitro-L-arginine methyl ester
<b>SGLT2</b>	sodium glucose cotransporter
<b>snRNA-seq</b>	single-nuclei RNA-sequencing
<b>TAC</b>	transverse aortic constriction
<b>TNFα</b>	tumor necrotic factor alpha
<b>WT</b>	wild-type
<b>Xbp1</b>	X-box binding protein 1

unmet need, HFpEF is now recognized as the most significant challenge in cardiology today.<sup>6</sup>

Besides some common pathological features of left ventricular diastolic dysfunction<sup>7</sup> and hypertrophic remodeling, the clinical manifestations of HFpEF are actually quite heterogeneous and still poorly defined.<sup>8</sup> Comparing to the demographic features of HFrEF, patients with HFpEF are more often female and older.<sup>9</sup> In addition, they share highly prevalent comorbidities, including obesity/diabetes and hypertension,<sup>10,11</sup> as well as atrial fibrillation<sup>12</sup> and chronic kidney diseases, among others. Thus far, the molecular features that differentiate HFpEF versus HFrEF remain elusive, and much of the underlying mechanisms specifically implicated in HFpEF are yet to be established. Recent advances in both clinical and pre-clinical studies have provided some new insights into the pathogenesis of HFpEF.<sup>2,3,8,13–15</sup> It is now well recognized that the onset of HFpEF requires multiple pathological insults. Among them, hypertension and metabolic disorders are the 2 most prominent comorbidities observed in patients with HFpEF, and their combined impact on HFpEF development has now been recapitulated in pre-clinical models.<sup>15–17</sup> The pathological outcomes of either mechanical or metabolic stresses have been well studied separately. However, the molecular underpinning of their

synergistic interaction in the pathogenesis of HFpEF has not been clearly dissected. It is apparent that multiple cell types in intact heart tissue contribute to the pathological process of HFpEF.<sup>18–20</sup> The molecular pathways dysregulated in cardiomyocytes that contribute to HFpEF remain to be fully unmasked.

In the current study, we aim to capture and dissect the synergistic impact of mechanical and metabolic stresses in cardiomyocytes by applying pressure overload to hearts in either wild-type (WT) lean mice or B6.Cg-*Lep<sup>ob</sup>*/J (ob/ob) mice with preexisting obesity and metabolic disorders through transverse aortic constriction (TAC) surgery.<sup>21,22</sup> While the pressure-overloaded lean mice manifested characteristic features of HFrEF, the obese mice subjected to the same mechanical overload developed heart failure more characteristic of HFpEF. Single-nuclei transcriptome profiling of heart tissues revealed specific transcriptome signatures in the cardiomyocytes associated with HFpEF versus HFrEF phenotypes and uncovered an unexpected role of cardiomyocyte-specific glucagon signaling in HFpEF development. Using both genetic and pharmacological tools, we further demonstrated that inhibition of glucagon receptor signaling exerts a therapeutic effect in experimental HFpEF.

## METHODS AND MATERIALS

### Data Availability Statement

The data that support the findings of this study are available from the corresponding author upon reasonable request.

Detailed methods and materials, including detailed statistical methods and the original uncropped gels for immunoblot results, are provided as part of [Supplemental Material](#). Representative images or gels used in the final figures were selected from multiple samples, mostly at random (such as histological sections) or cropped for clarity of presentation (such as immunoblot blot gels). All RNA-seq data sets are deposited with GEO accession number GSE270896.

## RESULTS

### Pathogenic Interaction Between Metabolic Disorder and Pressure Overload in Mice

To determine the functional interaction between metabolic and mechanical stresses in the heart, we applied medium grade pressure overload in 8-week-old C57Bl/6J lean mice and age matched obese ob/ob mice by performing TAC surgery using a 25G size needle (Figure 1A). The status of obesity and hyperglycemia in the ob/ob mice was demonstrated by weight measurements and glucose tolerance tests<sup>23</sup> (Figure S1). Longitudinal assessment of cardiac function was performed by serial echocardiogram (Figures S2 and S3). After 6 weeks of pressure overload, the lean mice began to show a significant

decrease in ejection fraction (Figure S3A; Figure 1B, 1D, and 1F). In contrast, the ob/ob mice showed a preserved ejection fraction for the entire duration of the experiment (Figure S3B; Figure 1C, 1E, and 1F). Instead, the ob/ob mice developed significant deterioration in diastolic function in response to pressure overload, as manifested in altered E/e' ratio (Figures S2, S3C, and S3D; Figure 1G). Using more sensitive cardiac strain imaging analysis, we detected no significant changes in radial strain or diastolic strain or their corresponding strain rates in the post-TAC lean mice relative to the sham group at 3 weeks post-TAC (Figure 1H through 1K). However, the ob/ob mice showed significant decreases in radial strain PK%, diastolic radial strain PK%, and their corresponding strain rates at this time point (Figure 1H through 1K). Therefore, the ob/ob mice developed significant contractile dysfunction in response to pressure overload, particularly at diastolic level, with a preserved ejection fraction. By invasive hemodynamic analysis at 10 weeks postpressure overload (Figure 2A through 2D), we observed that TAC significantly increased end-systolic pressure in both lean and ob/ob mice (Figure 2E). The obese mice exhibited a trend of higher left ventricular end-diastolic pressure over the lean mice under either sham or post-TAC conditions (Figure 2F). In addition, the ob/ob mice developed higher levels of  $dP/dt_{max}$  and  $dP/dt_{min}$ , likely due to increased stiffness and myocyte hypertrophy (Figure 2G and 2H). Indeed, the ob/ob mice showed significantly elevated end-diastolic pressure-volume relationship slope and relaxation time ( $\tau$ ) over the lean mice following pressure overload, both key hemodynamic parameters for myocardial stiffness (Figure 2I and 2J). Overall, the obese mice displayed worse diastolic dysfunction in response to pressure overload in comparison with the lean mice, albeit with a preserved ejection fraction.

At the tissue level, the ob/ob mice developed more severe cardiac hypertrophy, as demonstrated by higher heart weight (Figure 3A), left ventricle weight (Figure 3B), and enlarged cardiomyocyte sizes (Figure 3C and 3D). The ob/ob mice also had a significantly higher level of pulmonary edema (Figure 3E). Treadmill testing revealed that 10 weeks of TAC significantly decreased exercise capacity in lean WT mice by 13% compared with the Sham. On the contrary, the ob/ob mice had markedly reduced exercise capacity at basal compared with the lean mice, which further deteriorated by 44% after pressure overload (Figure 3F). Furthermore, the pressure-overloaded ob/ob mouse hearts also displayed elevated oxidative stress in myocardium (Figure 3G and 3H). Lastly, pressure overload induced the expression of *Nppb* in both lean and ob/ob hearts. However, the pressure-overload triggered *Nppb* induction was much higher in the lean mice than in the ob/ob mice, consistent with some clinical observations that pro-brain natriuretic protein may not be a useful biomarker to distinguish HFpEF from HFrEF<sup>24,25</sup> (Figure 3I).

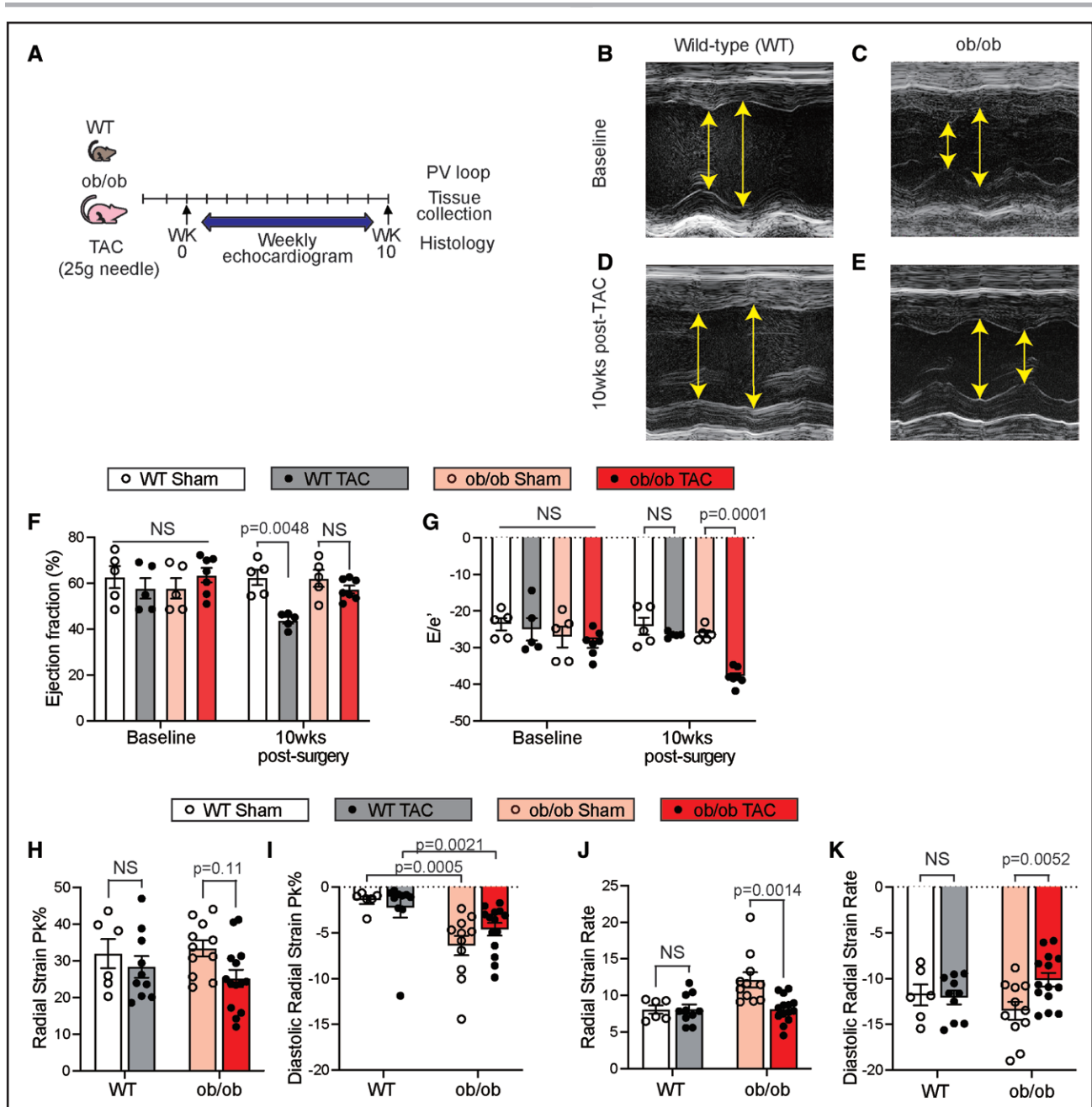


**Figure 1. Moderate pressure overload-induced diastolic cardiac dysfunction in obese mice.**

**A**, Schematic view of experimental design. **B** through **E**, Representative echocardiogram images (M-Mode) for wild-type (WT) and ob/ob mice at baseline and 10 weeks post-TAC. **F**, Ejection fraction of WT and ob/ob mice at baseline and 10 weeks post-TAC.  $P=0.015$  between WT sham baseline and WT-TAC 10 weeks postsurgery. **G**, Mitral valve  $E/e'$  of WT and ob/ob mice at baseline and 10 weeks post-TAC.  $P=0.0057$  between ob/ob TAC baseline and ob/ob TAC 10 weeks postsurgery. **H**, Radial strain PK% of WT and ob/ob mice at 3 weeks postsham or TAC operation. **I**, Diastolic radial strain PK% of WT and ob/ob mice 3 weeks postsham or TAC operation. **J**, Radial strain rate in WT and ob/ob mice 3 weeks postsham or TAC operation. **K**, Diastolic radial strain rate of WT and ob/ob mice 3 weeks postsham or TAC operation. ART-ANOVA followed by Tukey's test was used for statistical analysis for **F** through **K**. ART indicates aligned rank transform; and TAC, transverse aortic constriction.

## Metabolic Disorder Aggravated Pressure Overload-Induced Cardiac Fibrosis and Inflammation

Clinically, heart failure with preserved ejection fraction is associated with systematic and local inflammation as well as fibrotic remodeling in cardiac tissue.<sup>26–29</sup> At the

histological level, ob/ob hearts showed elevated cardiac fibrosis without concurrent pressure overload, and the degree of fibrotic remodeling further deteriorated after pressure overload (Figure S4). At the molecular level, pressure-overloaded ob/ob hearts showed higher expression of genes associated with inflammation and fibrosis, including C-reaction protein, tumor necrotic

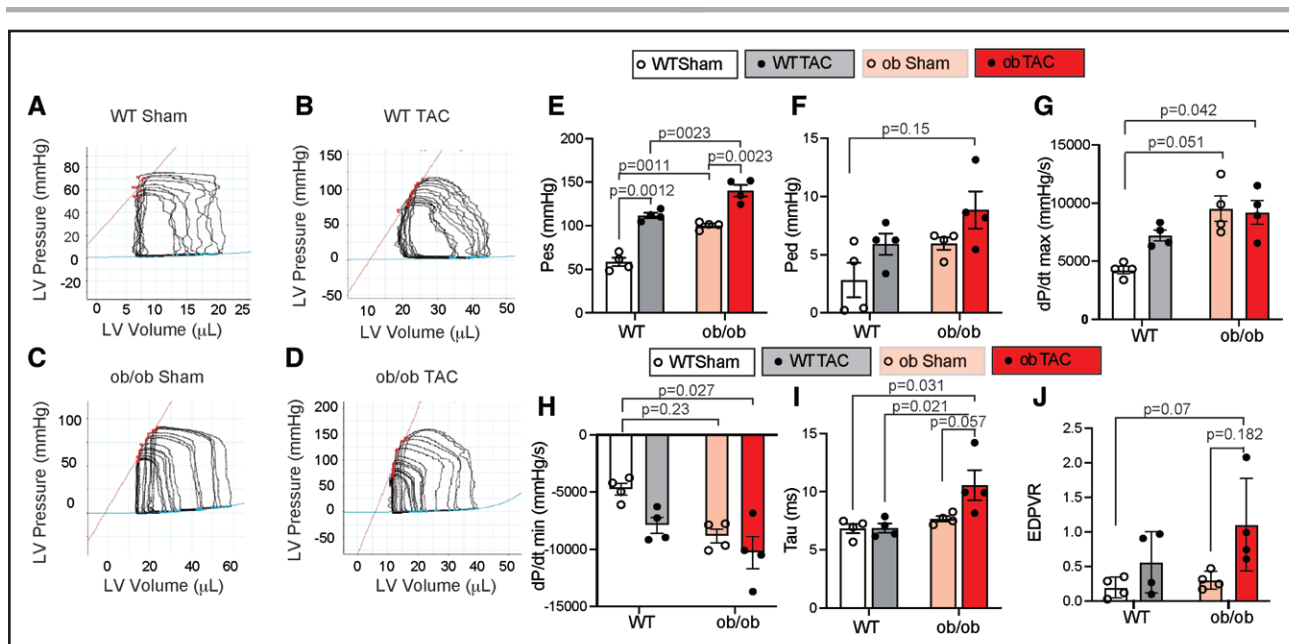


**Figure 2. Hemodynamic evidence of diastolic heart failure in pressure-overloaded obese mice.**

**A** through **D**, Pressure-volume loops for WT sham (**A**), WT-TAC (**B**), ob/ob sham (**C**), and ob/ob TAC (**D**) mice 10 weeks post-operation. **E**, Catheter analysis of end-systolic pressure (Pes) in WT and ob/ob mice 10 weeks postsham or TAC operation. **F**, Catheter analysis of end-diastolic pressure (Ped) in WT and ob/ob mice 10 weeks postsham or TAC operation. **G**, Catheter analysis of dP/dt max in WT and ob/ob mice 10 weeks postsham or TAC operation. **H**, Catheter analysis of dP/dt min in WT and ob/ob mice 10 weeks postsham or TAC operation. **I**, Relaxation time constant (tau) in WT and ob/ob mice 10 weeks post-TAC or sham operation. **J**, End-diastolic pressure-volume relationship (EDPVR) in WT and ob/ob mice 10 weeks post-TAC or sham operation. ART-ANOVA followed by Tukey's test was used for statistical analysis for **E** through **J**. ART indicates aligned rank transform; LV, left ventricle; TAC, transverse aortic constriction; and WT, wild-type.

factor alpha (*Tnfa*), collagen (*Col3a1*), and prothrombin (*F2*; Figure 3J through 3M). Consistent with previous observations in a mouse model of HFpEF,<sup>16,30</sup> the spliced Xbp1 (X-box binding protein 1) level (a measurement of IRE1 $\alpha$  [inositol-requiring enzyme 1 alpha] activity) was selectively reduced in the ob/ob post-TAC heart relative to the lean post-TAC mouse hearts, while other ER stress markers were not affected (Figure S5). In summary, pressure overload in combination with obesity led to significant remodeling characterized by fibrosis, inflammation, and oxidative stress, consistent with the common features observed in HFpEF.<sup>18,26,27,31–35</sup>

### Molecular Signaling in Pressure-Overloaded Lean Versus Obese Heart

We performed both bulk and single-nuclei RNA-sequencing (snRNA-seq) analyses from the 4 experimental cohorts, including WT lean sham, lean post-TAC (WT-TAC), ob/ob sham, and ob/ob post-TAC. Principal component analysis from bulk RNA-seq of the left ventricles (Figure 4A) revealed a global shift in transcriptome profiles in the ob/ob heart compared with the lean mouse heart under basal conditions. In contrast, a transcriptome shift at a different dimension was also observed in the lean mouse heart after pressure overload (mostly reflected in the first principal component for mechanical stress). Interestingly, the global transcriptome

profile in the ob/ob mouse heart with pressure overload was significantly different from either ob/ob at baseline or lean post-TAC but appeared to be shifted at a converging point between the 2 (Figure 4A), suggesting potential contributions from metabolic and mechanical stresses. To investigate the specific pathways affected in cardiomyocytes, nuclei from 2 male hearts of each experimental group at 8 weeks post-TAC/Sham were harvested and subjected to snRNA-seq. The major cardiac cell types were identified based on clustering and marker genes, including endothelial cells, fibroblasts, cardiomyocytes, and macrophages (Figure S6; Figure 4B). Gene expression profiles in cardiomyocytes were compared between lean and ob/ob hearts before and after pressure overload (Figure 4C). Among the significantly upregulated pathways in the ob/ob post-TAC versus lean post-TAC cardiomyocytes, insulin resistance and glucagon signaling were identified as the most enriched pathways (Figure 4D). For the downregulated genes, the top-ranked pathways differentiating the 2 conditions were mitochondrial respiratory activities and cardiac contractility (Figure S7). The top 10 upregulated genes in ob/ob post-TAC versus lean post-TAC cardiomyocytes were instead markedly downregulated in lean post-TAC versus lean-sham (Figure 4E). In contrast, the top 10 downregulated genes in ob/ob post-TAC versus lean post-TAC were markedly induced in lean post-TAC versus lean-sham (Figure 4F). Similarly, opposite changes in

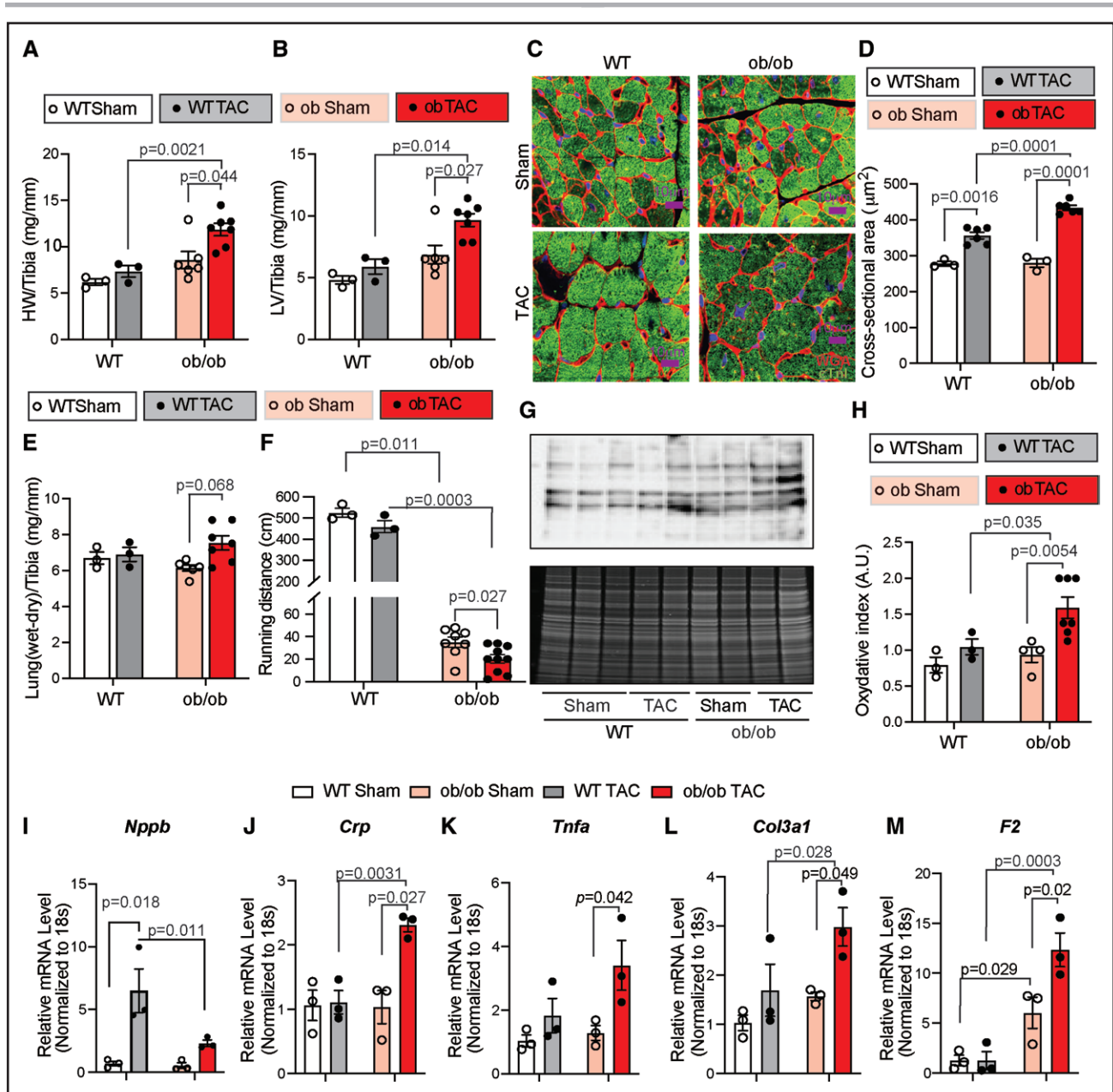


**Figure 3. Cardiac remodeling in obese and pressure-overloaded mice.**

**A**, Heart weight/tibia ratio of WT and ob/ob mice 10 weeks postsham or TAC operation. **B**, Left ventricle weight/tibia ratio of WT and ob/ob mice 10 weeks postsham or TAC operation. **C** and **D**, Cardiac hypertrophic status measured by wheat germ agglutinin (WGA) staining (**C**) and cross-sectional area quantification (**D**) for WT and ob/ob 10 weeks postsham or TAC operation, n=3 for each sham and n=6 for each TAC group. **E**, Wet minus dry lung weight to tibia length ratio in WT and ob/ob mice 10 weeks postsham or TAC operation. **F**, Running distances measured from exercise endurance tests for WT and ob/ob mice 10 weeks post-TAC or sham operation. **G** and **H**, Representative images of oxyblot (top) and oriole staining (bottom) for protein loading control (**G**) and quantification (**H**) from WT and ob/ob cardiac tissue 10 weeks postsham or TAC operation. ART-ANOVA followed by Tukey's test was used for statistical analysis for (**A**), (**B**), (**D**), (**E**), (**F**), and (**H**). **I** through **M**, Quantitative RT-PCR analysis of *Nppb* (**I**), *Crp* (**J**), *Tnfa* (**K**), *Col3a1* (**L**), and *F2* (**M**) expression in WT and ob/ob mouse hearts 10 weeks postsham or TAC operation. Two-way ANOVA followed by an LSD test was used for statistical analysis. ART indicates aligned rank transform; HW, heart weight; RT-PCR, reverse transcription polymerase chain reaction; TAC, transverse aortic constriction; and WT, wild-type.

expression were observed for top genes from the insulin resistance and glucagon signaling pathways (Figure 4G and 4H). Therefore, single-nuclei transcriptome profiling revealed diametric effects of pressure overload in lean versus obese cardiomyocytes, particularly affecting insulin and glucagon signaling. This differential impact on

insulin signaling was consistent with differential patterns of gene expression downstream of insulin signaling, including *Irs1*, *Rictor*, *Mtor*, and *Rptor* (Figure 5A through 5D), as well as insulin stimulated AKT serine/threonine kinase 1 phosphorylation (Figure 5E and 5F). Hence, coexisting metabolic disorders may potentially contribute

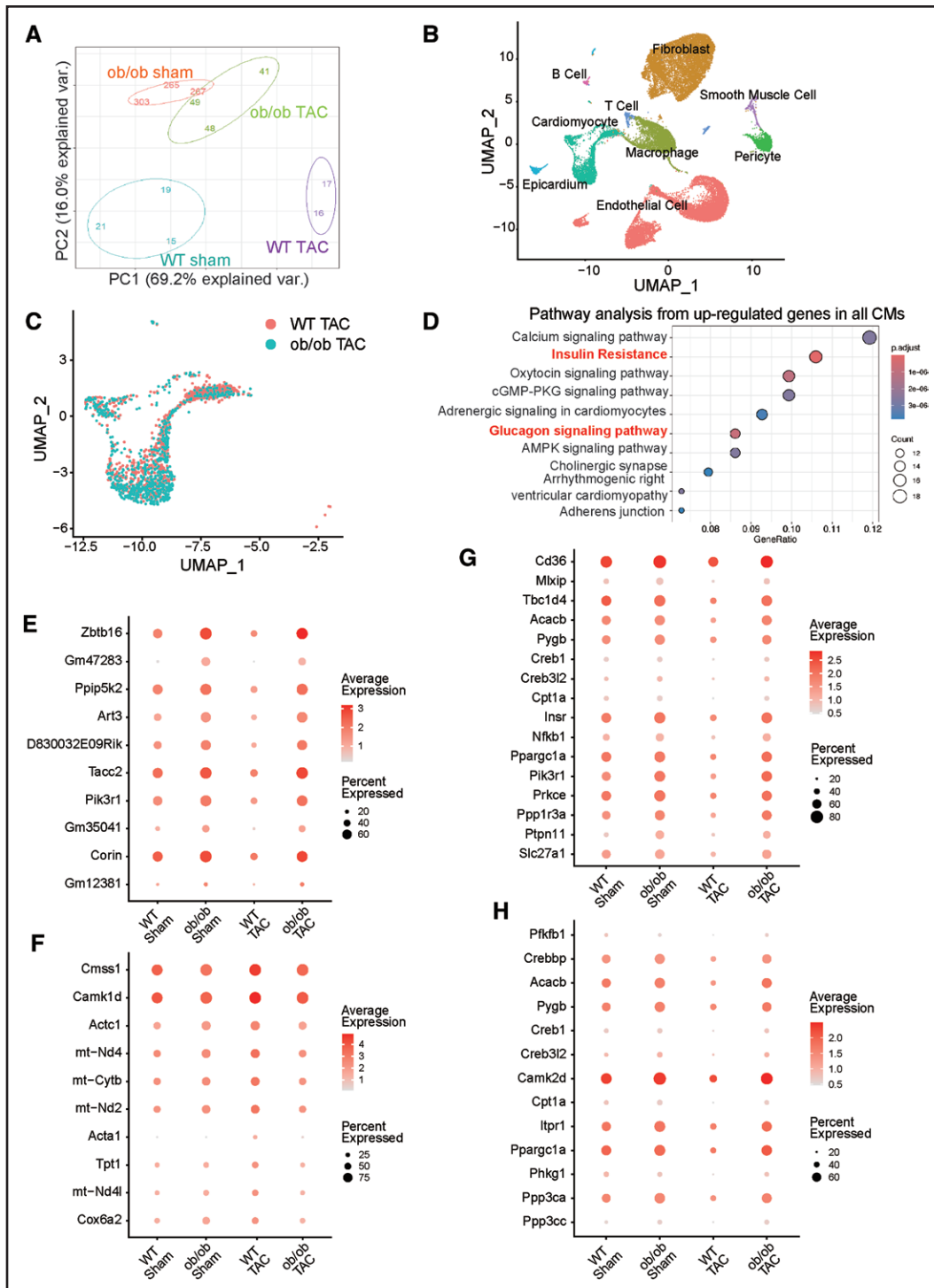


**Figure 4. Transcriptome signature in obese and pressure-overloaded mouse hearts.**

**A**, Transcriptome signature in lean vs ob/ob heart at basal vs postpressure overload using principal component analysis for all detected genes. **B**, The UMAP distribution of different cell types from the snRNA-seq analysis. **C**, The UMAP distribution of total cardiomyocytes from the aforementioned WT\_TAC (HFpEF) and Ob\_TAC (HFpEF) hearts. **D**, Top 10 KEGG pathways of up regulated genes in cardiomyocytes of Ob\_TAC vs WT\_TAC in the snRNA-seq data. **E**, Dot plots showing the expression profile of the top 10 upregulated genes of Ob\_TAC vs WT\_TAC. **F**, Dot plots showing the expression profile of the top 10 downregulated genes in Ob\_TAC vs WT\_TAC. **G**, Dot plots showing insulin resistance pathway genes (as shown in **D**) expression profiles across cardiomyocytes from the 4 conditions. **H**, Dot plots showing the glucagon signaling pathway genes (as shown in **D**) expression profile across cardiomyocytes from the 4 conditions. AMPK indicates adenosine monophosphate activated protein kinase; CM, cardiomyocyte; HFpEF, heart failure with preserved ejection fraction; HFrEF, heart failure with reduced ejection fraction; KEGG, Kyoto Encyclopedia of Genes and Genomes; TAC, transverse aortic constriction; UMAP, Uniform Manifold Approximation and Projection; and WT, wild-type.



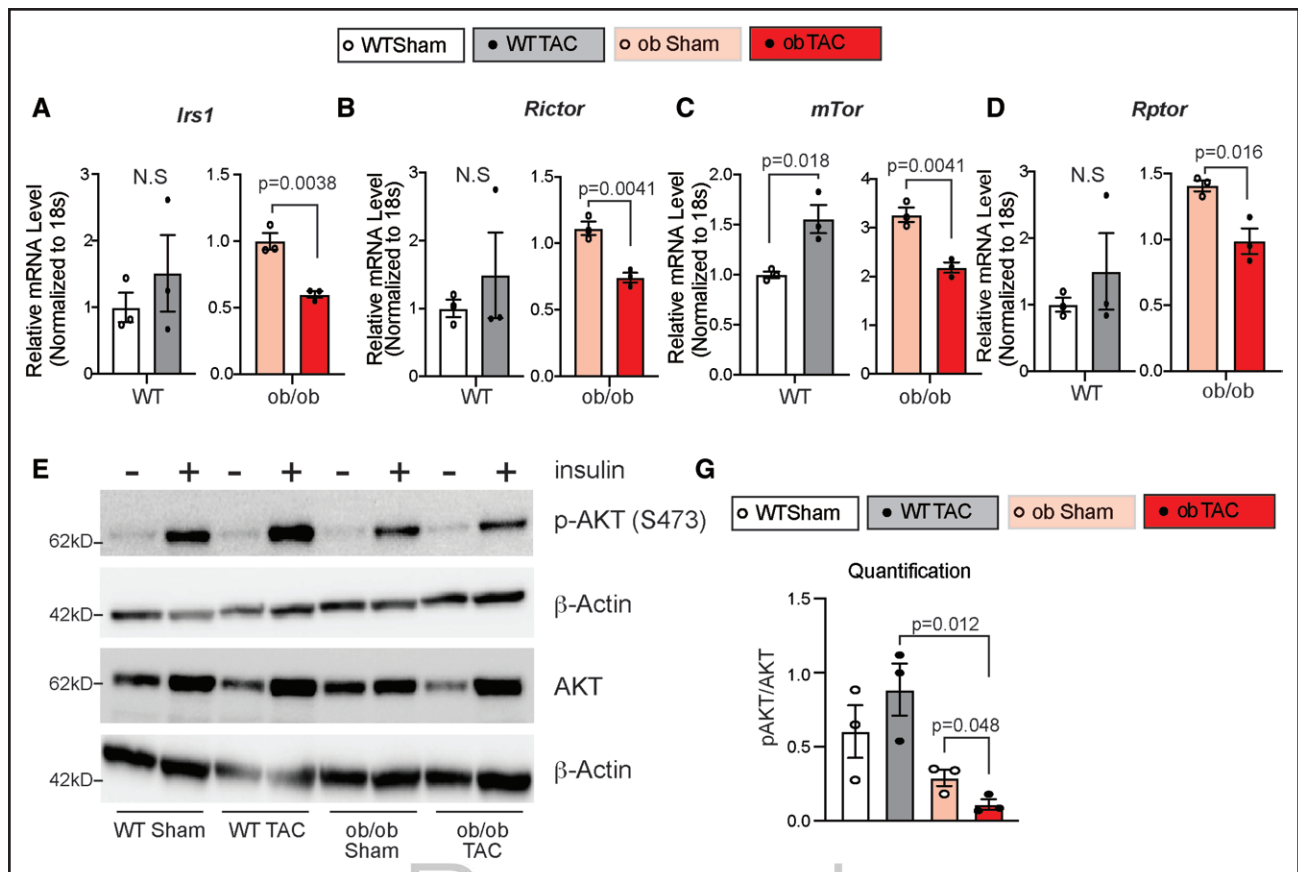


**Figure 5. Pressure overload exacerbated insulin signaling defects in the obese mouse heart.**

**A** through **D**, Quantitative RT-PCR analysis of gene expression for (**A**) *Irs1*, (**B**) *Rictor*, (**C**) *Mtor*, and (**D**) *Rptor* in WT and ob/ob mice cardiac tissue 10 weeks postsham or TAC operation. Student *t* test was used for statistical analysis. **E** and **F**, Representative immunoblot (**E**) and quantification (**F**) of downstream proteins of insulin signaling pathway in WT and ob/ob mice hearts postsham or TAC operation with and without insulin treatment. ART-ANOVA, followed by Tukey test, was used for statistical analysis. ART indicates aligned rank transform; RT-PCR, real-time polymerase chain reaction; TAC, transverse aortic constriction; and WT, wild-type.

to and alter the deleterious effect of pressure overload by suppressing insulin signaling while augmenting glucagon signaling in the heart.

### Glucagon Receptor Inhibition Blocks the Onset of Pathological Manifestation of HFpEF

Glucagon-mediated signaling has been demonstrated to have a direct and pathogenic role in heart,<sup>36,37</sup> but its impact on HFpEF has not been reported. REMD2.59 is a highly specific and potent glucagon receptor antagonist.<sup>37</sup> Weekly injection of REMD2.59 or placebo was administered in ob/ob sham or TAC-operated mice at the onset of pressure overload for 10 weeks (Figure 6A). REMD2.59 significantly improved systemic glucose metabolism (Figure S8). Echocardiography showed REMD2.59-treated ob/ob mice had improved diastolic function without significant changes in ejection fraction (Figure S9; Figure 6B and 6C) and reduced cardiac hypertrophy (Figure 6D through 6G). However, there was only a trend in *Nppb* reduction and exercise capacity improvement in the REMD2.59-treated groups (Figure S10).

Notably, while the combined stress of obesity and pressure overload altered the expression of insulin signaling, including *Irs1*, *Rictor*, *Mtor*, and *Rptor*, treatment with REMD2.59 reversed these changes (Figure 6H through 6K). Lastly, we observed a modest decrease in oxidative stress, but not nitrosative stress, in myocardial tissue treated with REMD2.59 (Figure 6L; Figure S11).

### Glucagon Receptor Antagonist as a Therapy for HFpEF

Next, we explored the therapeutic potential of targeting glucagon signaling as a treatment for established HFpEF in a mouse model that recapitulates many of the clinical features of the disease.<sup>16</sup> We treated 8-week-old lean mice with a high-fat diet (HFD) together with *N* $\omega$ -nitro-L-arginine methyl ester (L-NAME) for 9 weeks to allow the development of HFpEF phenotype as previously described.<sup>16</sup> These HFpEF mice were then randomized for weekly systemic administration of REMD2.59 or vehicle for an additional 5 weeks (Figure 7A). REMD2.59 administration attenuated HFD-induced

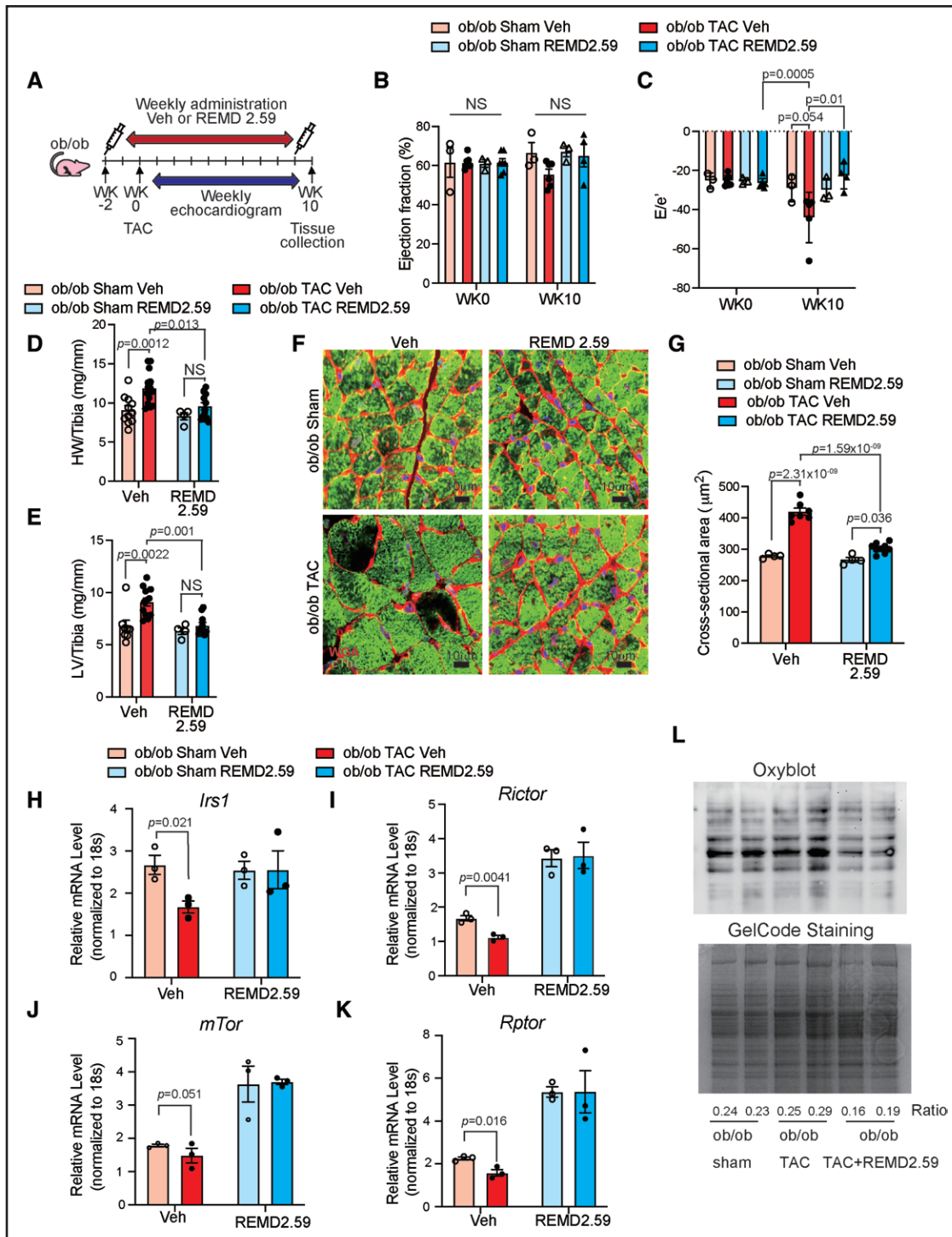


**Figure 6. Glucagon receptor antagonism improves diastolic cardiac function in obese and pressure-overloaded mice.**

**A**, Schematic view of experimental design. **B**, Ejection fraction of ob/ob animals treated with vehicle or REMD2.59 at indicated time points measured by echocardiography. **C**, Mitral valve E/e' ratio of ob/ob animals treated with vehicle or REMD2.59 at indicated time points measured by echocardiography. **D**, Heart weight/tibia ratio in ob/ob animals treated with vehicle or REMD2.59 10 weeks postsham or TAC operation. **E**, Left ventricle weight/tibia ratio of ob/ob mice post-TAC or sham operation with different injection. **F** and **G**, Representative wheat germ agglutinin (WGA) staining (**F**) and cross-sectional area quantification (**G**) for cardiomyocytes in the left ventricle of ob/ob mice with REMD2.59 or vehicle treatment 10 weeks postsham or TAC operation. n=4 for each sham group, n=7 for TAC+Veh, and n=9 for TAC+REMD2.59. ART-ANOVA followed by Tukey's test was used for statistical analysis for (**B**), (**C**), (**D**), (**E**), and (**G**). **H** through **K**, Real-time PCR analysis of *Irs1* (**H**), *Rictor* (**I**), *mTOR* (**J**), and *Rptor* (**K**) expression in vehicle or REMD2.59-treated ob/ob mice. n=3 biological samples for each group. Two-way ANOVA, followed by Tukey test, was used for statistical analysis. **L**, Oxyblot analysis for left ventricle samples from ob/ob sham, ob/ob TAC, and ob/ob TAC with REMD2.59 injection. ART indicates aligned rank transform; HW, heart weight; LV, left ventricle; PCR, polymerase chain reaction; and TAC, transverse aortic constriction.

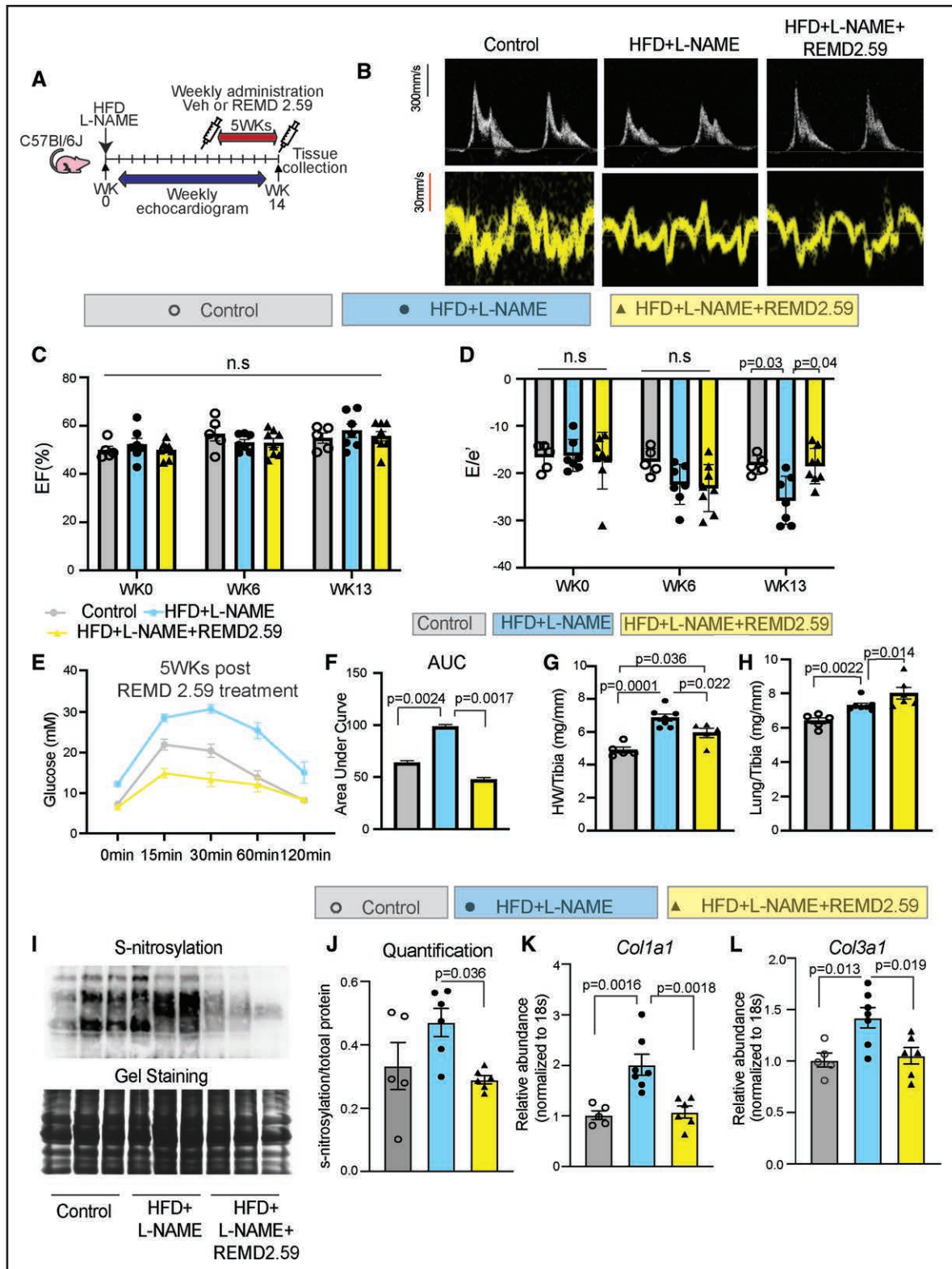


**Figure 7. Glucagon receptor antagonism improves diastolic cardiac function in nitrosative stress-induced HFpEF mice.**

**A**, Schematic view of experimental design. Eight-week-old C57Bl/6J mice were treated with a high-fat diet (HFD) and L-NAME for 9 weeks before being injected with vehicle or REMD2.59 daily for 5 weeks. **B**, Representative echo images showing mitral valve and tissue Doppler. **C**, Ejection fraction for control, HFD+L-NAME, or HFD+L-NAME+REMD2.59 mice at indicated time points. **D**, E/e' ratio for control, HFD+L-NAME, or HFD+L-NAME+REMD2.59 mice at indicated time points. **E** and **F**, Glucose tolerance test (**E**) and area under the curve (**F**) performed in control, HFD+L-NAME, and HFD+L-NAME+REMD2.59-treated mice 5 weeks post-treatment.  $P=0.022$  for (**E**) using Friedman test. One-way ANOVA, followed by Tukey test, was used for statistical analysis for (**F**). **G** and **H**, Heart weight/tibia (**G**) and lung weight/tibia (**H**) ratio among the 3 different treated groups. **I** and **J**, S-nitrosylation blot (**I**) and quantification (**J**) for left ventricle tissues among the 3 different treated (Continued)

body weight gain (Figure S12). Remarkably, REMD2.59 treatment significantly reversed HFD+L-NAME-induced cardiac diastolic dysfunction without impact on ejection fraction based on serial echocardiography analysis (Figure 7B through 7D, Figures S13 and S14). Administration of REMD2.59 significantly improved the glucose homeostasis measured by the glucose tolerance test (Figure 7E and 7F). Treatment with REMD2.59 also attenuated cardiac hypertrophy, leading to a reduced heart weight/tibia ratio (Figure 7G), without improving the status of pulmonary congestion (Figure 7H). At molecular levels, we did not observe significant changes in expression for hypertrophic marker gene, including atrial natriuretic peptide and brain natriuretic protein (Figure S15A through S15C). Neither did we observe any significant improvement in exercise endurance level based on treadmill analysis (Figure S15D). However, we have indeed observed a significant decrease in nitrosative stress status upon REMD 2.59 treatment (Figure 7I and 7J). Lastly, cardiac fibrotic marker genes, including Col1a1 (collagen 1 alpha 1) and Col3a1 (collagen 3 alpha 1), were significantly reduced (Figure 7K and 7L). Taken together, systemic inhibition of glucagon signaling using REMD2.59 improved cardiac diastolic function in established HFpEF.

### Cardiomyocyte-Specific Contribution of Glucagon Signaling to Cardiac Diastolic Dysfunction

Identification of glucagon signaling changes in cardiomyocytes through snRNA analysis raised an interesting question on its systemic versus cardiomyocyte-specific role in the pathogenesis of HFpEF. To investigate the cardiomyocyte cell-autonomous effect of glucagon signaling in heart failure, we generated a mouse line with tamoxifen-inducible cardiomyocyte-specific knockout glucagon receptor (*Gcgr-cKO*), which carries both alleles of the floxed *Gcgr* allele (*Gcgr<sup>fl/fl</sup>*)<sup>38</sup> and cardiomyocyte-specific inducible Cre ( $\alpha$ MHC-MCM).<sup>39,40</sup> Following tamoxifen treatment to enable Cre-mediated inactivation of *Gcgr* in cardiomyocytes (Figure 8A and 8B), the mice were fed with a HFD for 4 weeks, followed by pressure overload, while the HFD was continued for an additional 8 weeks. Inactivation of the *Gcgr* gene in cardiomyocytes does not significantly impact the bodyweight gain following the HFD challenge (Figure 8C). The ejection fraction was not affected across all genotypes and treatment conditions (Figure 8D). However, the diastolic function in the *Gcgr-cKO* hearts

was significantly improved versus the control (*Gcgr<sup>fl/fl</sup>*) mice (Figure 8E), supporting a direct contribution of cardiomyocyte GCGR signaling to cardiac diastolic dysfunction. Inactivation of *Gcgr* does not impact the heart or left ventricle size based on tissue weights (Figure 8F and 8G) but modestly improves the exercise intolerance level measured by running distance (Figure 8H). Although we did not observe any significant changes in oxidative stress or nitrosative stress status in the *Gcgr-cKO* mouse hearts compared with their controls (Figure S16), we observed a significant reduction of stress-induced pathological marker gene expression in the *Gcgr-cKO* heart (Figure 8I through 8K). Interestingly, cardiac specific deletion of *Gcgr* also marginally improved systemic glucose homeostasis under chronic HFD (Figure 8L and 8M; Figure S17), pointing to the potential impact of cardiac glucagon signaling on systemic metabolic regulation. This line of genetic evidence further demonstrated the therapeutic potential of glucagon receptor antagonism to improve diastolic dysfunction associated with HFpEF.



### DISCUSSION

In this study, we investigated the potential synergistic interactions between mechanical overload and metabolic stress in the heart by combining moderate pressure overload in lean versus obese mice with diabetes. We found pressure overload led to divergent pathological outcomes in lean versus diabetic/obese mice. While the lean mice developed prototypic features of HFrEF following pressure overload, the obese mice developed significant diastolic dysfunction and hypertrophic remodeling with preserved ejection fraction. Transcriptome profiling clearly indicated divergent molecular impacts from mechanical versus metabolic stresses in the heart and the interaction between the 2 in generating the cardiac pathological features associated with HFpEF. Using snRNA-seq profiling, we further identified distinct molecular signatures in the pressure-overloaded cardiomyocytes of obese versus lean mice. Pathway enrichment analysis revealed specific induction of insulin resistance and glucagon signaling in the cardiomyocytes of pressure-overloaded obese mice. The pathogenic significance of this finding was demonstrated by a significant improvement in cardiac diastolic function and remodeling from genetic or pharmacological inhibition of the glucagon receptor in 2 independent preclinical models of HFpEF.

The phenotypic outcome observed from simultaneous mechanic and metabolic overload supports the

**Figure 7 Continued.** groups. **K** and **L**, Real-time PCR analysis of Col1a1 (**K**) and Col3a1 (**L**) among the control, HFD+L-NAME, and HFD+L-NAME+REMD2.59-treated groups. N=5 to 8 in each group. ART-ANOVA, followed by Tukey test, was used for statistical analysis for (**C**), (**D**), (**G**), (**H**), and (**J**) One-way ANOVA, followed by Tukey test, was used for statistical analysis for (**K**) and (**L**). ART indicates aligned rank transform; EF, ejection fraction; HFpEF, heart failure with preserved ejection fraction; HW, heart weight; L-NAME, N $\omega$ -nitro-L-arginine methyl ester; and PCR, polymerase chain reaction.

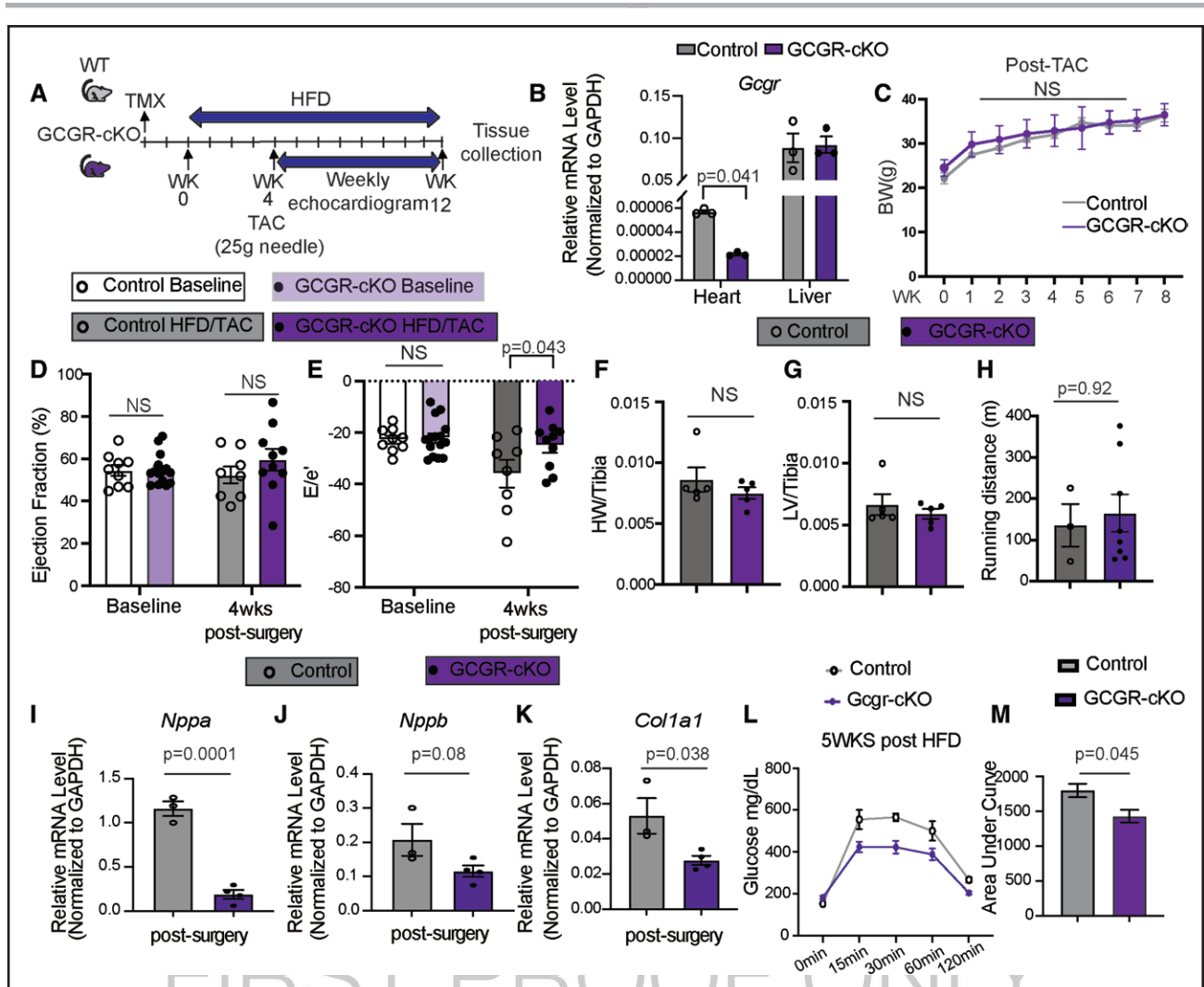


**Figure 8. Glucagon receptor cardiomyocyte-specific deletion impacts diastolic dysfunction in obese and pressure-overloaded mice.**

**A**, Three-month-old mice with *Gcgr<sup>fl/fl;mer-cre-mer</sup>* (*Gcgr-cKO*) or control genotype (*Gcgr<sup>fl/fl</sup>*) were treated with TMX for 2 weeks before being treated with HFD. Four weeks later, TAC was performed with a 25G needle and followed up for 8 weeks. **B**, Expression of *Gcgr* mRNA in the heart and liver tissues of control and *Gcgr-cKO* mice was measured by qRT-PCR. Two-way ANOVA, followed by Tukey test, was used for statistical analysis. **C**, Bodyweights of male control and *Gcgr-cKO* mice at different time points post-TAC. Repeated ANOVA was used for statistical analysis. **D**, Ejection fraction. **E**, E/e' measured by echocardiogram. **F**, Heart weight normalized to tibial length. **G**, Left ventricle weight normalized to tibial length. **H**, Running distance on treadmill for control and *Gcgr-cKO* mice 8 weeks post-TAC. **I** through **K**, Relative expression levels of cardiac genes including *Nppa* (**I**), *Nppb* (**J**), and *Col1a1* (**K**) normalized to GAPDH in post-TAC control and *Gcgr-cKO* hearts; Student *t* test was used for statistical analysis. **L** and **M**, Glucose tolerance test (**L**,  $P=0.003$ ) and area under the curve (**M**) for control and *Gcgr-cKO* male mice 5 weeks post-HFD. Repeated ANOVA was used for statistical analysis for (**L**). Two-way ANOVA, followed by Tukey test, was used for statistical analysis for (**B**), (**D**), and (**E**). Student *t* test was used for analysis for (**I**), (**J**), (**K**), and (**M**). Data in (**F**), (**G**), and (**H**) were analyzed via Mann-Whitney *U* test. BW indicates body weight; HFD, high-fat diet; GAPDH, glyceraldehyde 3-phosphate dehydrogenase; qRT-PCR, quantitative real-time polymerase chain reaction; TAC, transverse aortic constriction; and TMX, tamoxifen.

well-established paradigm underlying the pathogenesis of HFpEF, which is clearly a complex syndrome caused by multiple insults, such as hypertension and metabolic disorders associated with obesity and insulin resistance.<sup>3,18,41</sup> The pathological features observed in a pressure-overloaded heart with an obese/diabetic background are consistent with the results observed in a heart treated with a HFD plus L-NAME.<sup>16</sup> Consistently, Xbp1 activity was also reduced in the ob/ob post-TAC hearts, implicating it as a potential converging signaling in the

pathogenic process of HFpEF. The shared efficacy of glucagon receptor antagonist in 2 preclinical models of HFpEF further supports the validity of glucagon signaling as an important underlying mechanism for the pathogenesis of the disease. Therefore, pressure overload in obese mice might be useful as an additional preclinical model of HFpEF, along with several others reported in rodents and large animals.<sup>42–44</sup>

Although the insulin resistance signal is to be expected considering the presence of global insulin

resistance in the ob/ob mice, the significant induction of glucagon signaling in obese and pressure-overloaded cardiomyocytes is somewhat unexpected and intriguing. Glucagon's canonical function is to counterbalance the glucose-lowering effects of insulin in the liver and pancreas.<sup>45</sup> Although the expression level of glucagon receptor (GCGR) in the heart is low relative, recent studies suggest that the cell-autonomous effect of glucagon and glucagon receptor-mediated signaling in cardiomyocytes can significantly aggravate cardiac dysfunction and remodeling in injured heart.<sup>38</sup> Other studies have also suggested glucagon receptor antagonism could improve cardiac function in diabetic mice by promoting the AMPK (adenosine monophosphate activated protein kinase) signaling pathway.<sup>46</sup> Our results indicate that cardiomyocyte-specific glucagon receptor signaling has a clear impact on cardiac diastolic dysfunction and molecular reprogramming. However, the extent of hypertrophy was not significantly impacted by glucagon receptor inactivation in cardiomyocytes. In contrast, when the glucagon receptor antagonist was administered through systemic delivery, both diastolic dysfunction and cardiac hypertrophy were markedly reversed in association with the improvement of systemic glucose metabolism. These results indicate that the cardiomyocyte-specific impact of glucagon may be limited to contractile regulation, particularly at a diastolic level, while systemic glucagon signaling is also important for hypertrophic remodeling.

The underlying mechanism for glucagon-mediated contractile regulation in cardiomyocytes is entirely unknown and should be further explored. More importantly, SGLT2 (sodium glucose cotransporter) inhibition is an emerging new therapy for heart failure and has demonstrated exciting cardioprotective effects against adverse outcomes in patients with both HFrEF and HFpEF.<sup>47,48</sup> However, SGLT2 inhibition leads to elevated glucagon production,<sup>49,50</sup> which can be of questionable benefit for heart failure efficacy. Glucagon antagonism is an emerging new treatment currently being tested in clinics for type 1 diabetes with promising preliminary outcomes.<sup>51</sup> Therefore, our preclinical data reported here would support the consideration of a combination therapy of glucagon receptor antagonism and SGLT2 inhibition or GLP-1 (glucagon-like peptide-1) receptor agonism for HFpEF associated with both hypertension and obesity/diabetes.<sup>52</sup>

The results from our current study should also be interpreted with full recognition of the following limitations. The study was performed on mostly young animals, missing a key risk factor for HFpEF, that is, aging, and transcriptome profiling was only performed on male samples. The contribution of other nonmyocyte cardiac components, such as fibroblasts, endothelial cells, and macrophages, is yet to be further studied. In particular, the cell-cell interaction in response to mechanical and

metabolic stresses may play important roles in the synergistic outcome observed in intact hearts.<sup>53–56</sup> Our study was performed over a 10-week period of time, still relatively short compared with the long-term therapeutic interventions required for clinical applications. Lastly, the key mechanistic question of downstream targets of glucagon signaling in cardiomyocytes remains to be elucidated. Clinically, HFpEF has always been recognized as a multi-organ syndrome, and the remarkable benefits observed from REMD2.59 treatment may be contributed by its effects on multiple organs outside the heart. Nevertheless, the current study revealed an important synergistic impact of metabolic and mechanical stresses in cardiomyocytes. Uncovering the underlying mechanisms will be key to better understanding the complex pathogenic process of heart failure with preexisting metabolic disorders.

## ARTICLE INFORMATION

Received April 7, 2024; revision received July 1, 2024; accepted July 8, 2024.

### Affiliations

Department of Pharmacology and Systems Physiology, University of Cincinnati, OH (C.G., T.L.). Department of Cardiovascular Medicine, Third Affiliated Hospital of Sun Yat-Sen University, Guangzhou, Guangdong, China (Z.X.). Signature Research Program in Cardiovascular and Metabolic Diseases, DukeNUS School of Medicine, Singapore (Y.L., Meng Wang, S.R., Y.W.). Department of Cardiology, Renmin Hospital of Wuhan University, China (Menglong Wang, J.L.). School of Medicine and Public Health, University of Wisconsin, Madison (N.C.). REMD Biotherapeutics, Camarillo, CA (Y.H.). Lunenfeld Tanenbaum Research Institute, Mt. Sinai Hospital, Toronto, Ontario, Canada (D.J.D.). Computational Medicine Program and Department of Human Genetics, University of North Carolina at Chapel Hill (C.D.R.). Division of Cardiology, Department of Medicine, David Geffen School of Medicine at University of California, Los Angeles, and the VA Greater Los Angeles Healthcare System (T.Y.). Division of Endocrinology, Department of medicine, David Geffen School of Medicine, University of California, Los Angeles (J.H.). Department of Medicine, Duke University School of Medicine, Durham, NC (Y.W.).

### Sources of Funding

D.J. Drucker is supported by a Banting and Best Diabetes Centre chair in Incretin Biology, a Sinai Health Novo Nordisk Foundation Fund in Regulatory Peptides, and Canadian Institutes of Health Research grant 154321. Y. Wang and C. Gao are supported by PR191670 DoD/CDMRP. J. Huang is supported by American Heart Association 18POST33990469. C.D. Rau is supported by R01HL162363 and R00HL138301.

### Disclosures

D.J. Drucker has served as a consultant or speaker within the past 12 months to Altimmune, Amgen, Boehringer Ingelheim, Kallyope, Merck Research Laboratories, Novo Nordisk Inc, and Pfizer Inc. Neither D.J. Drucker or his family members hold issued stock directly or indirectly in any of these companies. He holds non-exercised options in Kallyope. The other authors report no conflicts.

### Supplemental Material

Expanded Materials and Methods  
Table S1  
Figures S1–S17  
Uncropped gel images of immunoblots  
References 59–64

## REFERENCES

1. Abudiyab MM, Redfield MM, Melenovsky V, Olson TP, Kass DA, Johnson BD, Borlaug BA. Cardiac output response to exercise in relation to metabolic demand in heart failure with preserved ejection fraction. *Eur J Heart Fail*. 2013;15:776–785. doi: 10.1093/eurjhf/hft026

2. Mishra S, Kass DA. Cellular and molecular pathobiology of heart failure with preserved ejection fraction. *Nat Rev Cardiol*. 2021;18:400–423. doi: 10.1038/s41569-020-00480-6
3. Zhan Q, Peng W, Wang S, Gao J. Heart failure with preserved ejection fraction: pathogenesis, diagnosis, exercise, and medical therapies. *J Cardiovasc Transl Res*. 2022;16:310–326. doi: 10.1007/s12265-022-10324-y
4. Oktay AA, Rich JD, Shah SJ. The emerging epidemic of heart failure with preserved ejection fraction. *Curr Heart Fail Rep*. 2013;10:401–410. doi: 10.1007/s11897-013-0155-7
5. Owan TE, Hodge DO, Herges RM, Jacobsen SJ, Roger VL, Redfield MM. Trends in prevalence and outcome of heart failure with preserved ejection fraction. *N Engl J Med*. 2006;355:251–259. doi: 10.1056/NEJMoa052256
6. Shah SJ, Borlaug BA, Kitzman DW, McCulloch AD, Blaxall BC, Agarwal R, Chirinos JA, Collins S, Deo RC, Gladwin MT, et al. Research priorities for heart failure with preserved ejection fraction: National Heart, Lung, and Blood Institute working group summary. *Circulation*. 2020;141:1001–1026. doi: 10.1161/CIRCULATIONAHA.119.041886
7. Paulus WJ, Tschöpe C. A novel paradigm for heart failure with preserved ejection fraction: comorbidities drive myocardial dysfunction and remodeling through coronary microvascular endothelial inflammation. *J Am Coll Cardiol*. 2013;62:263–271. doi: 10.1016/j.jacc.2013.02.092
8. Withaar C, Lam CSP, Schiattarella GG, de Boer RA, Meems LMG. Heart failure with preserved ejection fraction in humans and mice: embracing clinical complexity in mouse models. *Eur Heart J*. 2021;42:4420–4430. doi: 10.1093/eurheartj/ehab389
9. Hogg K, Swedberg K, McMurray J. Heart failure with preserved left ventricular systolic function: epidemiology, clinical characteristics, and prognosis. *J Am Coll Cardiol*. 2004;43:317–327. doi: 10.1016/j.jacc.2003.07.046
10. Carnes J, Gordon G. Biomarkers in heart failure with preserved ejection fraction: an update on progress and future challenges. *Heart Lung Circ*. 2020;29:62–68. doi: 10.1016/j.hlc.2019.05.180
11. Savji N, Meijers WC, Bartz TM, Bhamhani V, Cushman M, Naylor M, Kizer JR, Sarma A, Blaha MJ, Gansevoort RT, et al. The association of obesity and cardiometabolic traits with incident HFpEF and HFrEF. *JACC: Heart Failure*. 2018;6:701–709. doi: 10.1016/j.jchf.2018.05.018
12. Zakeri R, Chamberlain AM, Roger VL, Redfield MM. Temporal relationship and prognostic significance of atrial fibrillation in heart failure patients with preserved ejection fraction. *Circulation*. 2013;128:1085–1093. doi: 10.1161/CIRCULATIONAHA.113.001475
13. Lee CJ, Park S. Hypertension and heart failure with preserved ejection fraction. *Heart Fail Clin*. 2021;17:337–343. doi: 10.1016/j.hfc.2021.02.002
14. Tona F, Montisci R, Iop L, Civieri G. Role of coronary microvascular dysfunction in heart failure with preserved ejection fraction. *Rev Cardiovasc Med*. 2021;22:97–104. doi: 10.31083/j.rcm.2021.01.277
15. Withaar C, Meems LMG, Markousis-Mavrogenis G, Boogerd CJ, Silljé HHW, Schouten EM, Dokter MM, Voors AA, Westenbrink BD, Lam CSP, et al. The effects of liraglutide and dapagliflozin on cardiac function and structure in a multi-hit mouse model of heart failure with preserved ejection fraction. *Cardiovasc Res*. 2021;117:2108–2124. doi: 10.1093/cvr/cvaa256
16. Schiattarella GG, Altamirano F, Tong D, French KM, Villalobos E, Kim SY, Luo X, Jiang N, May HI, Wang ZV, et al. Nitrosative stress drives heart failure with preserved ejection fraction. *Nature*. 2019;568:351–356. doi: 10.1038/s41586-019-1100-z
17. Roh J, Hill JA, Singh A, Valero-Muñoz M, Sam F. Heart failure with preserved ejection fraction: heterogeneous syndrome, diverse preclinical models. *Circ Res*. 2022;130:1906–1925. doi: 10.1161/CIRCRESAHA.122.320257
18. Schiattarella GG, Alcaide P, Condorelli G, Gillette TG, Heymans S, Jones EAV, Kallikourdis M, Lichtman A, Marelli-Berg F, Shah S, et al. Immunometabolic mechanisms of heart failure with preserved ejection fraction. *Nat Cardiovasc Res*. 2022;1:211–222. doi: 10.1038/s44161-022-00032-w
19. Salvatore T, Galiero R, Caturano A, Vetrano E, Rinaldi L, Coviello F, Di Martino A, Albanese G, Colantuoni S, Medicamento G, et al. Dysregulated epicardial adipose tissue as a risk factor and potential therapeutic target of heart failure with preserved ejection fraction in diabetes. *Biomolecules*. 2022;12:176. doi: 10.3390/biom12020176
20. Weerts J, Mourmans SGJ, Barandiarán Aizpurua A, Schroen BLM, Knackstedt C, Eringa E, Houben A, van Empel VPM. The role of systemic microvascular dysfunction in heart failure with preserved ejection fraction. *Biomolecules*. 2022;12:278. doi: 10.3390/biom12020278
21. Gao C, Ren S, Lee JH, Qiu J, Chapski DJ, Rau CD, Zhou Y, Abdellatif M, Nakano A, Vondriska TM, et al. RBFOX1-mediated RNA splicing regulates cardiac hypertrophy and heart failure. *J Clin Invest*. 2016;126:195–206. doi: 10.1172/JCI84015
22. Suriano F, Vieira-Silva S, Falony G, Roumain M, Paquot A, Pelicaen R, Régnier M, Delzenne NM, Raes J, Muccioli GG, et al. Novel insights into the genetically obese (ob/ob) and diabetic (db/db) mice: two sides of the same coin. *Microbiome*. 2021;9:147. doi: 10.1186/s40168-021-01097-8
23. Sun H, Olson KC, Gao C, Prosdocimo DA, Zhou M, Wang Z, Jeyaraj D, Youn JY, Ren S, Liu Y, et al. Catabolic defect of branched-chain amino acids promotes heart failure. *Circulation*. 2016;133:2038–2049. doi: 10.1161/CIRCULATIONAHA.115.020226
24. Kim H, Jun DW, Cho YK, Nam CW, Han SW, Hur SH, Kim YN, Kim KB. The correlation of left atrial volume index to the level of N-terminal pro-BNP in heart failure with a preserved ejection fraction. *Echocardiogr*. 2008;25:961–967. doi: 10.1111/j.1540-8175.2008.00717.x
25. Djordjevic T, Arena R, Guazzi M, Popovic D. Prognostic value of NT-pro brain natriuretic peptide during exercise recovery in ischemic heart failure of reduced, midrange, and preserved ejection fraction. *J Cardiopulm Rehabil Prev*. 2021;41:282–287. doi: 10.1097/HCR.0000000000000531
26. van Empel V, Brunner-La Rocca HP. Inflammation in HFpEF: key or circumstantial? *Int J Cardiol*. 2015;189:259–263. doi: 10.1016/j.ijcard.2015.04.110
27. Schiattarella GG, Rodolico D, Hill JA. Metabolic inflammation in heart failure with preserved ejection fraction. *Cardiovasc Res*. 2021;117:423–434. doi: 10.1093/cvr/cvaa217
28. Bayes-Genis A, Cediñel G, Domingo M, Codina P, Santiago E, Lupón J. Biomarkers in heart failure with preserved ejection fraction. *Card Fail Rev*. 2022;8:e20. doi: 10.15420/cfr.2021.37
29. Daou D, Gillette TG, Hill JA. Inflammatory mechanisms in heart failure with preserved ejection fraction. *Physiology (Bethesda)*. 2023;38:0. doi: 10.1152/physiol.00004.2023
30. Schiattarella GG, Altamirano F, Kim SY, Tong D, Ferdous A, Pristine H, Dasgupta S, Wang X, French KM, Villalobos E, et al. Xbp1s-FoxO1 axis governs lipid accumulation and contractile performance in heart failure with preserved ejection fraction. *Nat Commun*. 2021;12:1684. doi: 10.1038/s41467-021-21931-9
31. Zhang N, Ma Q, You Y, Xia X, Xie C, Huang Y, Wang Z, Ye F, Yu Z, Xie X. CXCR4-dependent macrophage-to-fibroblast signaling contributes to cardiac diastolic dysfunction in heart failure with preserved ejection fraction. *Int J Biol Sci*. 2022;18:1271–1287. doi: 10.7150/ijbs.65802
32. Valero-Muñoz M, Oh A, Faudoa E, Bretón-Romero R, El Adili F, Bujor A, Sam F. Endothelial-mesenchymal transition in heart failure with a preserved ejection fraction: insights into the cardiorenal syndrome. *Circ Heart Fail*. 2021;14:e008372. doi: 10.1161/circheartfailure.121.008372
33. Kresoja KP, Rommel KR, Wachter R, Henger S, Besler C, Klötting N, Schnelle M, Hoffmann A, Büttner P, Ceglarek U, et al. Proteomics to improve phenotyping in obese patients with heart failure with preserved ejection fraction. *Eur J Heart Fail*. 2021;23:1633–1644. doi: 10.1002/ejhf.2291
34. Tallquist MD. Developmental pathways of cardiac fibroblasts. *Cold Spring Harb Perspect Biol*. 2020;12:a037184. doi: 10.1101/cshperspecta037184
35. Lewis GA, Schelbert EB, Williams SG, Cunningham C, Ahmed F, McDonagh TA, Miller CA. Biological phenotypes of heart failure with preserved ejection fraction. *J Am Coll Cardiol*. 2017;70:2186–2200. doi: 10.1016/j.jacc.2017.09.006
36. Karwi QG, Zhang L, Wagg CS, Wang W, Ghandi M, Thai D, Yan H, Ussher JR, Oudit GY, Lopaschuk GD. Targeting the glucagon receptor improves cardiac function and enhances insulin sensitivity following a myocardial infarction. *Cardiovasc Diabetol*. 2019;18:1. doi: 10.1186/s12933-019-0806-4
37. Gao C, Ren SV, Yu J, Baal U, Thai D, Lu J, Zeng C, Yan H, Wang Y. Glucagon receptor antagonism ameliorates progression of heart failure. *JACC Basic Transl Sci*. 2019;4:161–172. doi: 10.1016/j.jaccbts.2018.11.001
38. Ali S, Ussher JR, Baggio LL, Kabir MG, Charron MJ, Ilkayeva O, Newgard CB, Drucker DJ. Cardiomyocyte glucagon receptor signaling modulates outcomes in mice with experimental myocardial infarction. *Mol Metab*. 2015;4:132–143. doi: 10.1016/j.molmet.2014.11.005
39. Petrich BG, Molkentin JD, Wang Y. Temporal activation of c-Jun N-terminal kinase in adult transgenic heart via cre-loxP-mediated DNA recombination. *FASEB J*. 2003;17:749–751. doi: 10.1096/fj.02-0438fje
40. Sohal DS, Nghiem M, Crackower MA, Witt SA, Kimball TR, Tymitz KM, Penninger JM, Molkentin JD. Temporally regulated and tissue-specific gene manipulations in the adult and embryonic heart using a tamoxifen-inducible Cre protein. *Circ Res*. 2001;89:20–25. doi: 10.1161/011301.092687
41. Borlaug BA. The pathophysiology of heart failure with preserved ejection fraction. *Nat Rev Cardiol*. 2014;11:507–515. doi: 10.1038/nrcardio.2014.83
42. Regan JA, Mauro AG, Carbone S, Marchetti C, Gill R, Mezzaroma E, Raleigh JV, Salloum FN, Tassel BWV, Abbate A, et al. A mouse model of heart failure with preserved ejection fraction due to chronic

- infusion of a low suppressor dose of angiotensin II. *American Journal of Physiology-Heart and Circulatory Physiology*. 2015;309:H771–H778. doi: 10.1152/ajpheart.00282.2015
43. Marshall KD, Muller BN, Krenz M, Hanft LM, McDonald KS, Dellsperger KC, Emter CA. Heart failure with preserved ejection fraction: chronic low-intensity interval exercise training preserves myocardial O<sub>2</sub> balance and diastolic function. *J Appl Physiol (1985)*. 2013;114:131–147. doi: 10.1152/jappphysiol.01059.2012
  44. Olver TD, Edwards JC, Jurrissen TJ, Veteto AB, Jones JL, Gao C, Rau C, Warren CM, Klutho PJ, Alex L, et al. Western diet-fed, aortic-banded Ossabaw swine: a preclinical model of cardio-metabolic heart failure. *JACC Basic Transl Sci*. 2019;4:404–421. doi: 10.1016/j.jacbts.2019.02.004
  45. Wewer Albrechtsen NJ, Holst JJ, Cherrington AD, Finan B, Gluud LL, Dean ED, Campbell JE, Bloom SR, Tan TM, Knop FK, et al. 100 years of glucagon and 100 more. *Diabetologia*. 2023;66:1378–1394. doi: 10.1007/s00125-023-05947-y
  46. Sharma AX, Quittner-Strom EB, Lee Y, Johnson JA, Martin SA, Yu X, Li J, Lu J, Cai Z, Chen S, et al. Glucagon receptor antagonism improves glucose metabolism and cardiac function by promoting AMP-mediated protein kinase in diabetic mice. *Cell Rep*. 2018;22:1760–1773. doi: 10.1016/j.celrep.2018.01.065
  47. Usman MS, Siddiqi TJ, Anker SD, Bakris GL, Bhatt DL, Filippatos G, Fonarow GC, Greene SJ, Januzzi JL Jr, Khan MS, et al. Effect of SGLT2 inhibitors on cardiovascular outcomes across various patient populations. *J Am Coll Cardiol*. 2023;81:2377–2387. doi: 10.1016/j.jacc.2023.04.034
  48. Roy R, Vinjamuri S, Baskara S, Hafeez N, Meenashi Sundaram D, Patel T, Gudi TR, Vasavada AM. Sodium-glucose cotransporter-2 (SGLT-2) inhibitors in heart failure: an umbrella review. *Cureus*. 2023;15:e42113. doi: 10.7759/cureus.42113
  49. Bonner C, Kerr-Conte J, Gmyr V, Queniat G, Moerman E, Thévenet J, Beaucamps C, Delalleau N, Popescu I, Malaisse WJ, et al. Inhibition of the glucose transporter SGLT2 with dapagliflozin in pancreatic alpha cells triggers glucagon secretion. *Nat Med*. 2015;21:512–517. doi: 10.1038/nm.3828
  50. Ferrannini E, Muscelli E, Frascerra S, Baldi S, Mari A, Heise T, Broedl UC, Woerle HJ. Metabolic response to sodium-glucose cotransporter 2 inhibition in type 2 diabetic patients. *J Clin Invest*. 2014;124:499–508. doi: 10.1172/JCI72227
  51. Pettus J, Boeder SC, Christiansen MP, Denham DS, Bailey TS, Akturk HK, Klaff LJ, Rosenstock J, Cheng MHM, Bode BW, et al. Glucagon receptor antagonist volagidemab in type 1 diabetes: a 12-week, randomized, double-blind, phase 2 trial. *Nat Med*. 2022;28:2092–2099. doi: 10.1038/s41591-022-02011-x
  52. Kosiborod MN, Abildstrøm SZ, Borlaug BA, Butler J, Rasmussen S, Davies M, Hovingh GK, Kitzman DW, Lindegaard ML, Møller DV, et al. Semaglutide in patients with heart failure with preserved ejection fraction and obesity. *N Engl J Med*. 2023;389:1069. doi: 10.1056/NEJMoa2306963
  53. Wang L, Yang Y, Ma H, Xie Y, Xu J, Near D, Wang H, Garbutt T, Li Y, Liu J, et al. Single cell dual-omics reveals the transcriptomic and epigenomic diversity of cardiac non-myocytes. *Cardiovasc Res*. 2021;118:1548–1563. doi: 10.1093/cvr/cvab134
  54. Wang L, Yu P, Zhou B, Song J, Li Z, Zhang M, Guo G, Wang Y, Chen X, Han L, et al. Single-cell reconstruction of the adult human heart during heart failure and recovery reveals the cellular landscape underlying cardiac function. *Nat Cell Biol*. 2020;22:108–119. doi: 10.1038/s41556-019-0446-7
  55. Ren Z, Yu P, Li D, Li Z, Liao Y, Wang Y, Zhou B, Wang L. Single-cell reconstruction of progression trajectory reveals intervention principles in pathological cardiac hypertrophy. *Circulation*. 2020;141:1704–1719. doi: 10.1161/CIRCULATIONAHA.119.043053
  56. Paik DT, Cho S, Tian L, Chang HY, Wu JC. Single-cell RNA sequencing in cardiovascular development, disease and medicine. *Nat Rev Cardiol*. 2020;17:457–473. doi: 10.1038/s41569-020-0359-y
  57. Cui P, Xin H, Yao Y, Xiao S, Zhu F, Gong Z, Tang Z, Zhan Q, Qin W, Lai Y, et al. Human amnion-derived mesenchymal stem cells alleviate lung injury induced by white smoke inhalation in rats. *Stem Cell Res Ther*. 2018;9:101. doi: 10.1186/s13287-018-0856-7
  58. Takimoto E, Champion HC, Li M, Ren S, Rodriguez ER, Tavazzi B, Lazzarino G, Paolucci N, Gabrielson KL, Wang Y, et al. Oxidant stress from nitric oxide synthase-3 uncoupling stimulates cardiac pathologic remodeling from chronic pressure load. *J Clin Invest*. 2005;115:1221–1231. doi: 10.1172/JCI21968
  59. Yu JY, Cao N, Rau CD, Lee RP, Yang J, Flach RJR, Petersen L, Zhu C, Pak YL, Miller RA, et al. Cell-autonomous effect of cardiomyocyte branched-chain amino acid catabolism in heart failure in mice. *Acta Pharmacol Sin*. 2023;44:1380. doi: 10.1038/s41401-023-01076-9
  60. Bergmann O, Jovinge S. Isolation of cardiomyocyte nuclei from post-mortem tissue. *J Vis Exp*. 2012;10:4205. doi: 10.3791/4205
  61. Yokota T, McCourt J, Ma F, Ren S, Li S, Kim TH, Kurmangaliyev YZ, Nasiri R, Ahadian S, Nguyen T, et al. Type V collagen in scar tissue regulates the size of scar after heart injury. *Cell*. 2020;182:545–562.e23. doi: 10.1016/j.cell.2020.06.030
  62. Stuart T, Butler A, Hoffman P, Hafemeister C, Papalexi E, Mauck WM 3rd, Hao Y, Stoeckius M, Smibert P, Satija R. Comprehensive integration of single-cell data. *Cell*. 2019;177:1888–1902.e21. doi: 10.1016/j.cell.2019.05.031
  63. Butler A, Hoffman P, Smibert P, Papalexi E, Satija R. Integrating single-cell transcriptomic data across different conditions, technologies, and species. *Nat Biotechnol*. 2018;36:411–41+. doi: 10.1038/nbt.4096
  64. Huang da W, Sherman BT, Lempicki RA. Systematic and integrative analysis of large gene lists using DAVID bioinformatics resources. *Nat Protoc*. 2009;4:44–57. doi: 10.1038/nprot.2008.211